Stratiform Precipitation in Regions of Convection: A Meteorological Paradox?

Robert A. Houze Jr.
University of Washington, Seattle, Washington

ABSTRACT

It was once generally thought that stratiform precipitation was something occurring primarily, if not exclusively, in middle latitudes—in baroclinic cyclones and fronts. Early radar observations in the Tropics, however, showed large radar echoes composed of convective rain alongside stratiform precipitation, with the stratiform echoes covering great areas and accounting for a large portion of the tropical rainfall. These observations seemed paradoxical, since stratiform precipitation should not have been occurring in the Tropics, where baroclinic cyclones do not occur. Instead it was falling from convection-generated clouds, generally thought to be too violent to be compatible with the layered, gently settling behavior of stratiform precipitation.

In meteorology, convection is a dynamic concept; specifically, it is the rapid, efficient, vigorous overturning of the atmosphere required to neutralize an unstable vertical distribution of moist static energy. Most clouds in the Tropics are convection-generated cumulonimbus. These cumulonimbus clouds contain an evolving pattern of newer and older precipitation. The young portions of the cumulonimbus are too violent to produce stratiform precipitation. In young, vigorous convective regions of the cumulonimbus, precipitation particles increase their mass by collection of cloud water, and the particles fall out in heavy showers, which appear on radar as vertically oriented convective "cells." In regions of older convection, however, the vertical air motions are generally weaker, and the precipitation particles drift downward, with the particles increasing their mass by vapor diffusion. In these regions the radar echoes are stratiform, and typically these echoes occur adjacent to regions of younger convective showers. Thus, the stratiform and convective precipitation both occur within the same complex of convection-generated cumulonimbus cloud.

The feedbacks of the apparent heat source and moisture sink of tropical cumulonimbus convection to the large-scale dynamics of the atmosphere are distinctly separable by precipitation region. The part of the atmospheric response deriving from the areas of young, vigorous convective cells is two layered, with air converging into the active convection at low levels and diverging aloft. The older, weaker intermediary and stratiform precipitation areas induce a three-layered response, in which environmental air converges into the weak precipitation area at midlevels and diverges from it at lower and upper levels. If global precipitation data, such as that to be provided by the Tropical Rainfall Measuring Mission, are to be used to validate the heating patterns predicted by climate and general circulation models, algorithms must be applied to the precipitation data that will identify the two principal modes of heating, by separating the convective component of the precipitation from the remainder.

1. Traditions

"Stratiform precipitation" is a term often used in meteorology, yet the term is not defined in the *Glossary of Meteorology* (Huschke 1959), and its meaning and usage continually evolve. This article attempts to clarify the meaning of the term stratiform precipitation as it is currently used in the particular context of tropical meteorology and other regions where clouds are generated by atmospheric convection. Such an article would have seemed paradoxical, if not outright heretical, 30 years ago. Stratiform precipitation was generally thought to occur almost exclusively with fronts in midlatitude cyclones, where ice particles grow predominantly by vapor deposition in a deep, largely buoyantly stable nimbostratus cloud layer, drift down from upper levels, melt, and fall to the earth's surface as raindrops. Under certain cold conditions, the particles may never melt, and they reach the surface

Corresponding author address: Robert A. Houze Jr., Dept. of Atmospheric Sciences, University of Washington, Box 351640, Seattle, WA 98195.
E-mail: houze@atmos.washington.edu
In final form: 15 May 1997.

as snow rather than rain. In both cases, the upward air motion induces vapor deposition onto the growing ice particles but is weak enough to allow the particles to drift downward while they grow.

In a baroclinic cyclone, the widespread lifting producing the growth of the precipitation particles occurs in the regions of large-scale warm advection, which is concentrated in the vicinity of fronts. But stratiform precipitation also can occur in other large-scale and mesoscale dynamical settings, as long as there is ascent of saturated air weak enough to allow ice particles to fall out. In other words, the term stratiform precipitation designates a particular set of *microphysical* processes leading to the growth and fallout of the precipitation within the context of relatively gentle upward air motion; it does not refer to the specific dynamic cause of the vertical air motions within which the particles form, grow, and fall out.

Since the advent of weather radar in the late 1940s, the term stratiform has been used to describe precipitation as it appears in displays of radar data. Stratiform precipitation is fairly homogeneous in the horizontal, giving it a layered structure in vertical cross sections of radar reflectivity. In particular, it often exhibits a pronounced layer of high reflectivity called the "bright band," marking the layer in which the downward settling ice particles are melting (Battan 1973; Houze 1993).

Stratiform radar echoes contrast sharply with radar echoes from "convective precipitation," which appears on radar as "cells," another loosely defined term, apparently coined by Byers and Braham (1949) in their classic report on the Thunderstorm Project in Ohio and Florida. Cells are horizontally localized patches or cores of intense radar reflectivity. In a vertical cross section, a cell is a tall, thin column of high reflectivity. The orthogonality of its structure to that of a brightband echo often makes the convective "cell" quite recognizably distinct from "stratiform" precipitation on radar, and radar meteorologists have developed a tradition of speaking of radar echoes as convective or stratiform, according to whether they form patterns of vertically oriented intense cores or horizontal layers.

2. Radar observations in tropical field experiments: Emergence of a paradox

Because of its ubiquitous presence in baroclinic cyclones and fronts, and because of the dearth of meteorological observations in the Tropics up to the second half of this century, stratiform precipitation was thought to occur primarily, if not exclusively, in middle latitudes. As late as 1979, Herbert Riehl referred to tropical rain as "a cumulus regime, in contrast to the climates with stratus precipitation in higher latitudes." Riehl was correct in characterizing the Tropics as a "cumulus regime"; precipitating clouds in the Tropics are entirely convection-generated cumulonimbi, and baroclinic cyclones and fronts, indeed, do not occur in the Tropics. However, his statement does not recognize that stratiform precipitation is not restricted to higher-latitude clouds. It may *also* occur within the "cumulus regime."

In 1972, scientists aboard a Soviet research ship operating in the intertropical convergence zone (ITCZ) of the eastern tropical Atlantic took photographs of a radar display showing strong brightband echo (Shupiatsky et al. 1975, 1976a,b). In 1974, the Global Atmospheric Research Programme Atlantic Tropical Experiment (GATE) obtained more extensive radar observations in this region. One of the most significant findings of GATE was that the stratiform radar echoes, seen earlier by the Soviet scientists, had very strong bright bands and covered large areas (Houze 1975, 1977; Leary and Houze 1979a,b). About 40% of the rain falling on the ocean surface in GATE was stratiform (Cheng and Houze 1979; Leary 1984). These observations showed definitively that both convective and stratiform radar echoes occurred in a regime in which the clouds are generated entirely by atmospheric convection.

Since GATE, radar studies have confirmed, many times over, that a large component (~20%–50%) of tropical precipitation exhibits stratiform radar-echo structure [see Houze (1989) for a summary]. Moreover, the stratiform echoes usually coexist with cells within a "mesoscale" precipitation area, in which the rain covers contiguously a region 10–1000 km in horizontal dimension. Higher rainfall rates in these mesoscale precipitation areas are concentrated in the cells, but lighter stratiform rain covers most of the mesoscale area. A portion of the area is covered by echo of intermediate intensity, which may be either "convective" or "stratiform," depending on its vertical structure.

In addition to the purely tropical regimes, in which there is no chance of a baroclinic contribution to the precipitation processes, there have now been many studies recognizing the large presence of stratiform precipitation in convection-generated clouds and precipitation in midlatitude regimes (e.g., Rutledge and MacGorman 1988; Houze et al. 1990). The discussions

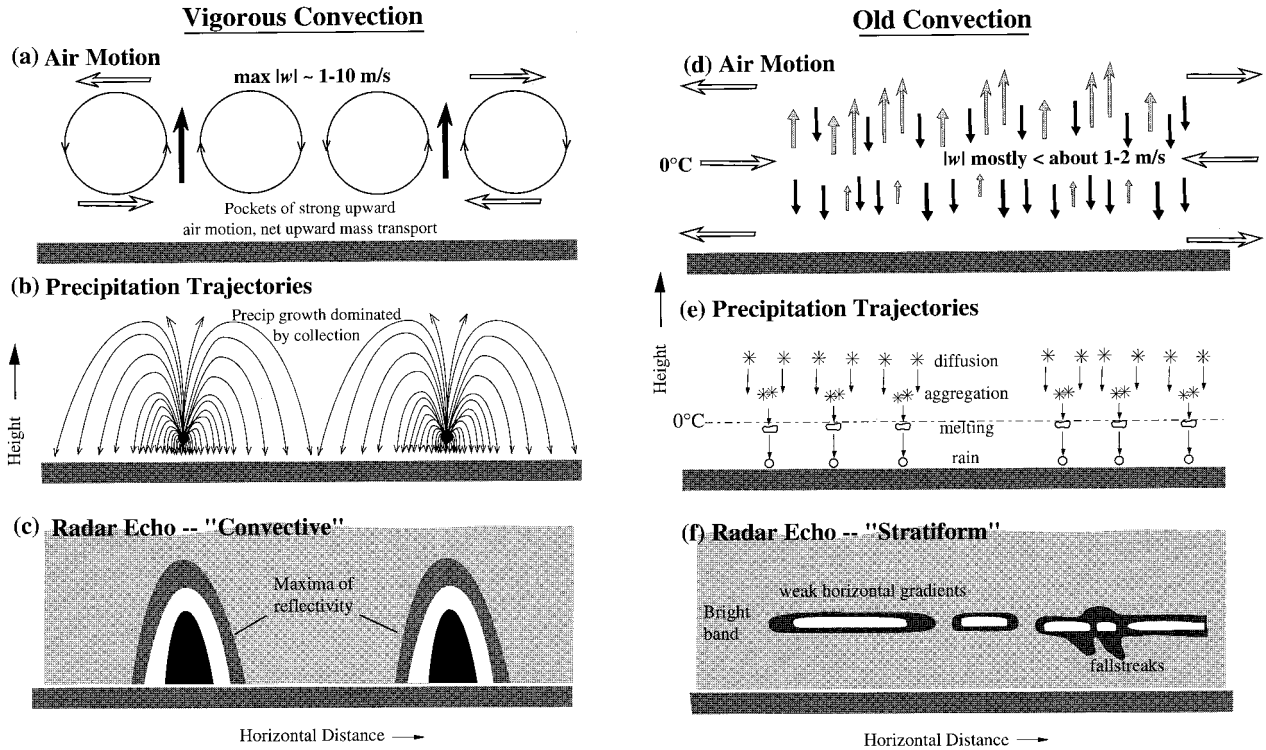

FIG. 1. Conceptual models of vertical cross sections through (a)–(c) young, vigorous precipitating convection and (d)–(f) old convection.

in this paper apply to both midlatitude and tropical convection.

3. Consistent terminology: The purpose of this paper

The fact that tropical precipitation, when observed by radar, has a substantial stratiform component has led to a terminology that seems contradictory, since the tropical atmosphere is clearly a region of *convection.* The term *convection* refers to the overturning of a fluid under gravity, and in the Tropics, nearly all precipitation (except part of that associated with tropical cyclones and possibly some orographic rain) is the product of atmospheric convection. However, the term stratiform, as defined above, is an adjective describing a set of microphysical processes that occur in weaker vertical air motions. Similarly, the term "convective" describes a *radar echo* from precipitation growing by the cloud-microphysical processes that attend the strong vertical air motions of young, active convection. Since stratiform radar echoes may be seen in an atmosphere of older convection, the terms stratiform (an adjective) and convection (a noun) are not mutually exclusive; stratiform describes the nature of some of the precipitation growth processes occurring in the region of convection, while the term convection alludes to the fluid dynamical origin of the air motions.

Henceforth, this paper, which is about tropical and other convection-generated precipitation, will use the noun *convection* to refer to an overturning fluid and the adjective *convective* to describe the precipitation (or radar echo) associated with young, active convection. The adjective *stratiform* will refer to precipitation occurring in older, less active convection and possessing radar echoes that have weak horizontal gradients and/or a bright band. Describing the *radar echoes* as being either convective or stratiform thus implies that the echoes depict precipitation in regions of stronger or weaker *air motions,* respectively, while at the same time recognizing that both the weaker and stronger air motions may arise from the process of convection. Convection can lead to cumulonimbus clouds, whose precipitation is partly convective and partly stratiform.[1] Figures 1 and 2 illustrate, in ideal-

[1]The stratiform precipitation could be considered to be falling from nimbostratus cumulonimbogenitus (precipitating stratiform cloud arising from cumulonimbus). Since such nimbostratus is usually a cloud deck currently or previously extruding out of the cumulonimbus, it seems artificial to call it a separate cloud. The author prefers to call the whole, single precipitating cloud entity a cumulonimbus.

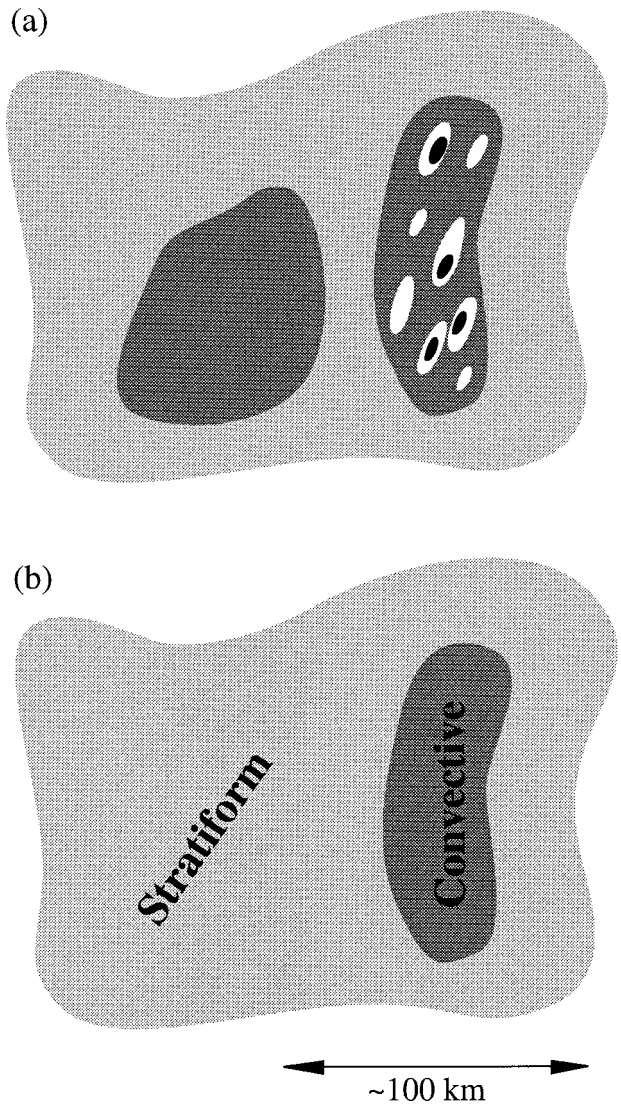

FIG. 2. Idealization of a horizontal map of radar reflectivity (a) divided into convective and (b) stratiform regions.

ized form, the terminology of this paper. The remainder of this paper delves further into this idealized picture in order to reach a deeper understanding of convection-generated precipitation and how to observe, describe, and interpret it.

4. What is convection?

To understand how both convective and stratiform precipitation can occur in response to convection, we should first review what we mean by convection in the context of cloud-formation processes. We say convection occurs when a fluid under gravity is heated from below or cooled from the top at such a rate that molecular diffusion cannot redistribute the modified density field fast enough so as to maintain equilibrium. The fluid layer then becomes buoyantly unstable and overturns macroscopically to stabilize the stratification of the density. One of the simplest examples is Benard convection in an incompressible fluid layer, where the fluid overturns by means of a field of geometrically simple vertically circulating elements. The atmospheric convection that produces cumulus and cumulonimbus clouds has the additional complications that air is a compressible fluid and contains water vapor, so overturning acts to neutralize the stratification of moist-static energy. Figure 1a shows atmospheric convection as a pattern of idealized vertically circulating elements, which are geometrically symmetric (like Benard cells) in the drawing, although in reality, the shapes of the overturning elements are highly modified by wind shear and by the interactions of the cloud and precipitation fields with the air motions. Asymmetries in the vertical structures of the cells do not affect the present discussion, which aims only to distinguish the terms "convective" and "stratiform" in describing precipitation. At the most basic level, it serves to keep to the symmetric idealization in Fig. 1a.

In atmospheric convection, water may condense and fall out. A saturated layer of air that is convectively overturning *and* precipitating, therefore, differs from a layer of Benard convection in that there must be a net upward transfer of air between the upper and lower boundaries of the fluid in order to account for the net condensation of water in the layer (as long as the rate of rise of temperature is less than the heating rate). The updrafts of the overturning cells must, therefore, transport more mass on average than do the downdrafts. Figures 3a and 3b summarize the effects of vertical mass transport in a region of active convective cells: net upward mass transport produces net latent heating at all levels (Fig. 3a), and mass continuity requires net horizontal convergence at low levels and divergence in the upper troposphere (Fig. 3b, open arrows in Fig. 1a). In the real atmosphere, a region of young, vigorous convection may not be completely saturated in its downdraft regions, but measurements confirm that the net mass divergence profiles are like that in Fig. 3b (e.g., Mapes and Houze 1995).

5. What is convective precipitation?

In deep precipitating atmospheric convection, the

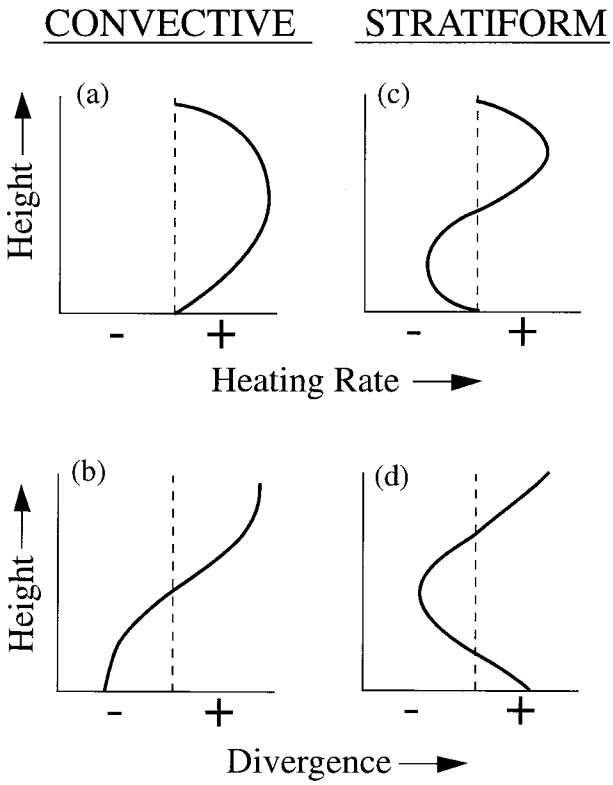

FIG. 3. Characteristic profiles of latent heating and horizontal mass divergence in convective and stratiform regions of tropical precipitation.

vertical velocities in the cores of the updrafts are several meters per second or greater. These strong updrafts condense vapor rapidly, producing large concentrations of cloud liquid water. Houghton (1968) pointed out that, in the presence of such strong updrafts, the dominant growth mechanism for precipitation particles is the collection of this cloud water by larger drops and/or ice particles sweeping out the cloud water in their fall paths. For growing water drops, this process is termed "coalescence"; in the case of collection by ice particles, it is known as "riming." Moreover, the strong updrafts allow for the larger particles to grow for a long period of time because they are carried upward relative to the earth, even though they are falling relative to the smaller cloud water droplets. This upward advection of the growing particles increases their residence time in cloud and thus their opportunities to collect cloud droplets. Figure 4 illustrates how, as a parcel of updraft air rises, the growing particles within it move up until they become large enough to fall relative to the air. At each successive height, some particles fall out of the parcel, while the remainder, which are not as heavy, are spread out laterally over an increasingly greater area by the divergent air flow as the rising, buoyant air parcel expands.

Since the bulk of the precipitation mass falls out within a few kilometers of the updraft centers, the radar reflectivity pattern associated with the convective air motions in Fig. 1a is a set of concentrated peaks of reflectivity, as shown in Fig. 1c. In plan view, the convective region appears in the radar echo as a field of localized reflectivity maxima (Fig. 2).

6. Stratiform precipitation in old convection

When atmospheric convection is young and vigorous, the precipitation occurs in cells, as indicated conceptually in Fig. 1a. However, as a region of convective cells weakens, the precipitation associated with the cells takes on a layered structure resembling that found in extratropical cyclonic precipitation. The upward vertical air motions in the region of weakened cells are strong enough to allow precipitation particles to grow by vapor diffusion but too weak to support high concentrations of cloud liquid water; therefore, growth by riming is not so effective as when the updrafts are stronger. In this respect, then, the region of weakened cells in a tropical cloud system resembles an extratropical cyclone.

Thus, when we divide the precipitation area of a convection-generated cloud system into convective and stratiform components (Fig. 2), we imply that the

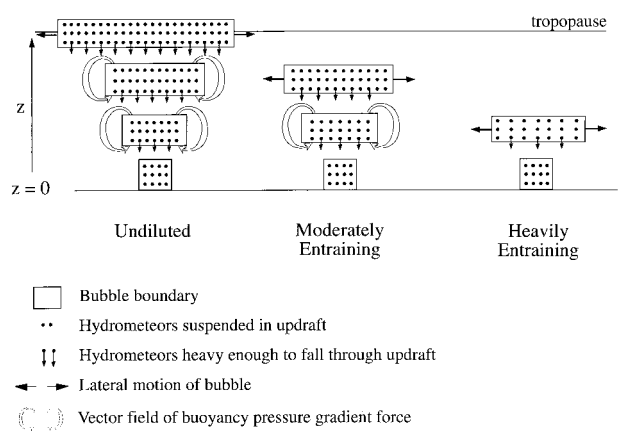

FIG. 4. Conceptual model of an updraft behaving like a buoyant bubble with different entrainment rates. Dots indicate hydrometeors suspended by updraft; downward-pointing arrows indicate particles heavy enough to fall through updraft; horizontal arrows indicate lateral spreading of bubble. Open arrows represent the vector field of the buoyancy pressure gradient force (as in Fig. 7.1 of Houze 1993). [From Yuter and Houze (1995c).]

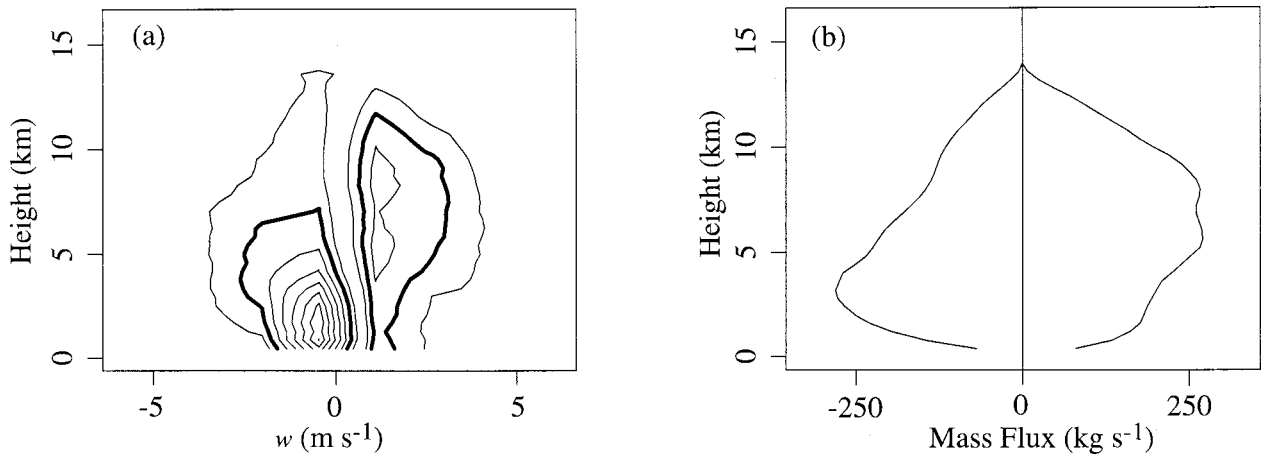

FIG. 5. (a) Vertical mass transport distribution by vertical velocity and (b) mass flux in a Florida cumulonimbus. Units of contours are [mass transport/($dw\ dz$)], where $dw = 1$ m s^{-1} and $dz = 0.4$ km. Contours are at intervals of 25×10^6 kg s^{-1}. [Adapted from Yuter and Houze (1995c).]

stratiform region is dominated by weaker air motions. These vertical air motions could be horizontally uniform across the stratiform region; however, they are usually variable in the horizontal. The requirements are only that there be net upward mass transport (to allow net condensation of vapor) in the cloud layer in which particles are growing on average and that the *ensemble* of vertical air motions in the cloud layer contain few if any upward velocities > 1 m s^{-1} (so that cloud liquid water production, and hence riming, is minimal and precipitation-sized particles are not advected upward, so as to overly disrupt the layered reflectivity pattern).

In a deep precipitating tropical cloud system, the "stratiform" precipitation region is typically a region of older convection (Fig. 1d). It is well known that in the older portions of a cumulonimbus, the lower troposphere is dominated by downdrafts, while the upper levels are dominated by weak updrafts. The upper levels are not wholly occupied by updrafts, nor are the lower levels wholly occupied by downdrafts. In the older part of the precipitation area of a Florida cumulonimbus, the vertical mass transport at upper levels was *net* upward (Fig. 5b), such that there was *net* growth of precipitation particles. However, the net upward mass transport at upper levels was the combined effect of an ensemble of vertical velocities, including some negative (downward) values, as shown by the distribution of the mass flux as a function of the vertical air velocity and height in Fig. 5a. However, updrafts < 2 m s^{-1} accounted for most of the upward mass transport; that is, nearly all of the volume of the storm at upper levels was occupied by air moving upward too slowly to overcome the downward fall velocities of precipitation particles. At these vertical air velocities, the condensed water is transferred to the growing ice particles almost entirely by vapor diffusion (Rutledge and Houze 1987), and the particles drift downward, as suggested by Fig. 1e. Below the 0°C level, the older precipitation regions are dominated by net downward motion (Houze 1989). Figure 5 shows that updrafts, mostly < 1.5 m s^{-1} in intensity, are interspersed among more predominantly downward air velocities. Zipser and LeMone (1980) and LeMone and Zipser (1980) described how research aircraft in GATE encountered both up- and downdrafts in ostensibly stratiform parts of tropical cumulonimbus.

When growing ice particles drift downward within the mid- to upper altitudes of a volume of air within a region of old convection such as that portrayed in Figs. 1d–f, distinct layers become evident via contrasting microphysical processes (Fig. 1e). At upper levels vapor diffusional growth is prevalent, and it is too cold for aggregation to occur. Empirical evidence indicates that aggregation occurs at ambient temperatures of 0° to ~ −15°C with the highest probability of aggregation in the temperature range of about 0 to ~ −5°C (Hobbs 1974, 641). Houze and Churchill (1987) confirmed this layering in tropical convection: they found large aggregates in this temperature layer among the particle images collected by aircraft in the stratiform regions of tropical convection over the Bay of Bengal in the Global Atmospheric Research Programme's Monsoon Experiment.

Displays of radar data enhance the layered appearance of stratiform precipitation because the reflectivity

of the melting snow is especially high for two reasons: 1) some of the melting particles are very large aggregates of ice crystals, and reflectivity is proportional to the sixth power of the particle dimension, and 2) the index of refraction of melting snowflakes is ~5 times greater than nonmelting ice. In addition, when the ice particles melt, their fall speeds increase by a factor of about 5, and the particles evacuate the melting layer rapidly in a vertically divergent fashion, producing a decreased concentration of particles below the melting layer. These factors combine to produce a pronounced bright band of enhanced reflectivity in a shallow layer centered just below the 0°C level (Fig. 1f).

The bright band is an unambiguous indicator of the presence of stratiform precipitation. However, *the absence of a bright band does not imply the absence of stratiform precipitation structure.* A bright band will not be observed unless the vertical resolution of the radar is sufficiently fine to delineate the band. Hence, the bright band is a property of the radar data; it is not a unique measure of the magnitude of the melting. A strong bright band only will appear if some of the melting particles are in the form of large aggregates. Temperature, ambient humidity, and crystal structures must all meet certain criteria for aggregation to occur. Aggregation of precipitating ice particles to form snowflakes does not add any mass to the precipitation, nor do the particles fall any faster once they have aggregated. Just as much latent heat is consumed in the melting, and the vertical flux of precipitation mass remains the same, regardless of whether or not the precipitating ice particles happen to aggregate to form large highly reflective particles and hence a bright band. Braun and Houze (1995) showed that the melting layer of a midlatitude mesoscale convective system was much more horizontally extensive than the radar bright band, which was present only in the part of the melting layer in which melting ice particles had aggregated to form very large snowflakes.

The presence of a bright band thus indicates the presence of a particular *type* of stratiform precipitation, namely that in which large aggregate snowflakes are among the melting particles. Since the ability to detect a bright band is a function of the characteristics of the radar rather than the storm, further caution is required, since the absence of a bright band does not indicate the absence of a layer of melting aggregates. Typically, a radar detects a bright band only at close range because the radar beam broadens with distance from the antenna and the melting layer is only ~0.5 km or less in depth.

The idealized bright band sketched in Fig. 1f is horizontally inhomogeneous, broken into several patches, and in one patch "fallstreaks" extend downward from the melting layer. Stratiform precipitation in tropical cumulonimbus usually occurs in regions where previously intense convection (like that depicted in Figs. 1a–c) has weakened. Since the previous convection was concentrated in cells, the resulting stratiform structure remains somewhat patchy, with highest reflectivities in the regions where convective cores once were vigorous; inspection of the high-resolution airborne radar data obtained in TOGA COARE[2] shows fallstreaks consistently in the locations of previously active convective cells (e.g., Yuter and Houze 1997a). The fallstreaks appear to occur where the remnant precipitation cores have not completely lost their identities, and since they are no longer part of an active convective cell, the remnant showers are distorted into tilted, bent fallstreaks by the ambient wind shear.

An alternative explanation for the fallstreaks is that an unstable layer produced by the latent cooling of the air by the melting leads to the formation of small, shallow convective cells in the melting layer. In this case, the fallstreaks would be similar to the "generating cells" seen in extratropical cyclonic precipitation (Marshall 1953). It is possible that the fallstreaks in tropical convection are a combination of remnant precipitation cores and overturning induced by melting cooling.

7. Dynamic implications of the stratiform component of tropical precipitation

Although vertical air motions are relatively weak in a stratiform region, the area covered by the stratiform precipitation can be much larger than that occupied by the active convective cells. A large portion of the time- and space-integrated vertical mass transport of the convection thus occurs in the older convection, that is, in the stratiform regions of cumulonimbus. For this reason, the stratiform regions of tropical convection have important dynamic implications.

[2]The Tropical Ocean Global Atmosphere Coupled Ocean–Atmosphere Response Experiment (TOGA COARE) was a large field experiment employing aircraft and ships to study the behavior of the atmosphere and ocean over the western tropical Pacific Ocean. The experiment ran from 1 November 1992 to 28 February 1993.

The large-scale environment responds to a convective system in a manner analogous to the way the water responds to a rock dropping into a pond. The water has to make way for the negatively buoyant rock accelerating downward through the fluid environment. The fluid adjusts to the sudden displacement of the water by a spectrum of gravity waves, which ripple away from the spot where the rock falls in the water.

In a similar way, a buoyant parcel of air pushes ambient air out of its path, and the surrounding atmosphere adjusts by sending out a spectrum of gravity waves, whose propagation speeds are proportional to their vertical wavelengths (Bretherton and Smolarkiewicz 1989; Mapes 1993). In a region of precipitating convection, there is a net positive buoyancy produced by the latent heat gained by air when precipitation falls out. The surrounding atmosphere adjusts to this generation of buoyancy by a spectrum of gravity waves (or more accurately bores) that have the net effect of displacing mass outside the convective region downward (Mapes 1993; Mapes and Houze 1995). The open arrows in Fig. 1a show the net result of this compensating downward displacement as a net horizontal transport of air from the environment into the active convective region (mass convergence) at lower levels and out of the region (mass divergence) at upper levels.

By the time the convective region is older, the net vertical mass transport in the lower levels of the precipitation region is downward (the negatively buoyant downdrafts begin to dominate over the updrafts). Net cooling occurs as a result of melting and evaporation at mid- to low levels during this stage (Fig. 3c), and horizontal divergence of air out of the storm must compensate the negative buoyancy in the lower troposphere of the rain areas (Fig. 3d, and the open arrows at low levels in Fig. 1d). Gravity waves that rearrange the environmental mass field around the stratiform rain areas must produce a net upward displacement of the environment to compensate the net horizontal mass divergence out of the old convective (i.e., stratiform) region at low levels.

The open arrows in Fig. 1d also show a net horizontal transport of air into the old convective region (mass convergence) at midlevels. This midlevel convergence compensates both the (net) positive buoyancy of the upper levels of the stratiform region and net negative buoyancy of the lower levels.

The most direct way to measure the adjustment of the large-scale environment to a region of convection is to measure the horizontal mass divergence into and out of the region. Accurate measurement of the outward normal component of the wind along the boundary of the volume of atmosphere containing the convection gives us this divergence, and in tropical field experiments, airborne Doppler radar data and rawinsondes have been used for this purpose. In TOGA COARE, aircraft Doppler radar provided 143 profiles of divergence around regions of precipitation. An example of the average of the profiles obtained on a flight sampling primarily convective precipitation showed convergence at low levels and divergence at upper levels (Fig. 6a), consistent with the open arrows in Fig. 1a. A flight sampling primarily old convection, indicated by the stratiform character of the radar echo, indicated strong convergence at midlevels (Fig. 6b), consistent with the open arrows in Fig. 1d. Figure 7 shows the grand mean profile of divergence, obtained by averaging all 143 samples obtained on flights in TOGA COARE. It represents the combination of active and old (stratiform) convection sampled on all the flights, over a 4-month period. The solid curve in Fig. 8 shows the profile of divergence obtained by averaging TOGA COARE rawinsonde data obtained around regions of satellite-observed active deep convection. It is consistent with the profile of divergence from the airborne Doppler radar (compare the profile in Fig. 7 with the solid curve in Fig. 8).

To determine how the large-scale atmosphere adjusts to a disturbance of its mass field by a region of deep convection, Mapes and Houze (1995) used the measured divergence profiles in Figs. 7 and 8 as input to a linear spectral primitive-equation model. In this model the divergence profile serves as a mass disturbance for the large-scale flow. The time-dependent flow predicted by the model, using the observed mass divergence profiles as input, indicates the modes of motion that develop when the large-scale atmosphere is perturbed by a divergence profile similar to that measured in the vicinity of the deep convection occurring in TOGA COARE. The calculation applies the observed divergence profile impulsively over a 140-km diameter region (a typical size of a deep convective precipitation area in TOGA COARE).

Two distinct modes dominate the model's large-scale response to the convection. The solutions of the equations are decomposed into vertical wavelength components, which correspond to the vertical wavelength components of the spectrally decomposed observed profile of divergence. The wave speed is directly proportional to the vertical wavelength, and Fig. 9a shows the magnitudes of the spectral coefficients

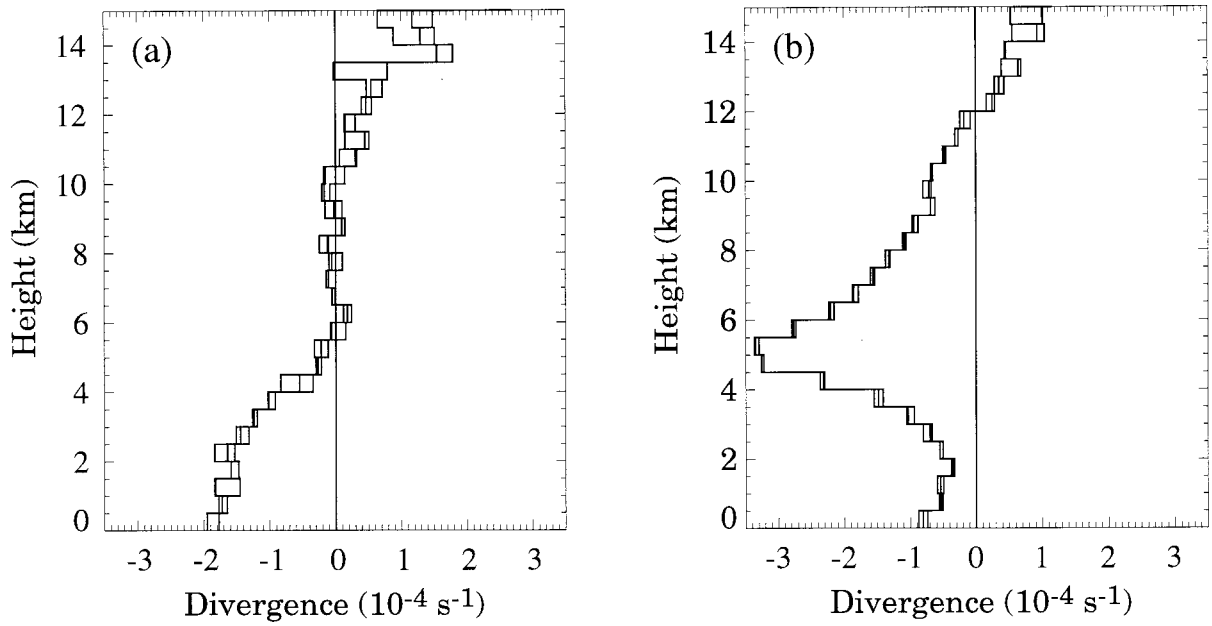

FIG. 6. Mean profiles of divergence measured by airborne Doppler radar in tropical precipitation over the western tropical Pacific during TOGA COARE: (a) from a flight in which most of the sampled precipitation was in a vigorously convective state (average of 13 samples obtained 15 December 1992); (b) from a flight in which most of the sampled precipitation was in a stratiform state (average of 15 samples obtained on 6 November 1992). All samples are for a region 30 km in diameter. The three lines in each plot are three independent radar measures for negligibly different geometry. [From Mapes and Houze (1995).]

of the divergence for each wave speed. The bigger the coefficient, the more that component of the divergence profiles accounts for the large-scale response to the convection. Figure 9a shows that the motions are dominated by bands of wave speeds centered on 52 and 23 m s^{-1}.

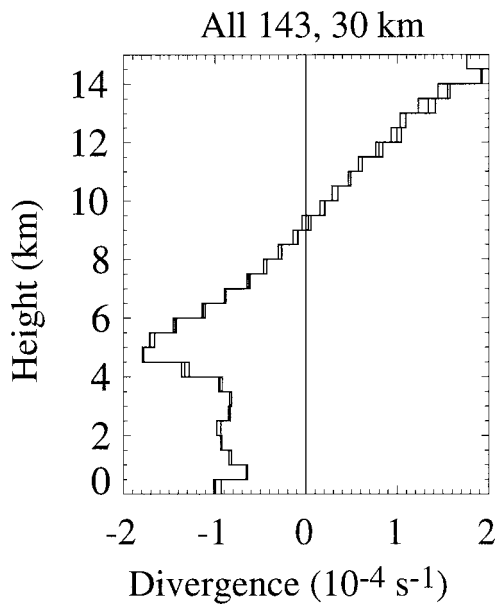

FIG. 7. Mean of all divergence profiles measured by airborne Doppler radar in tropical precipitation over the western tropical Pacific during TOGA COARE. The average is based on 143 samples, obtained on 10 different aircraft missions. [From Mapes and Houze (1995).]

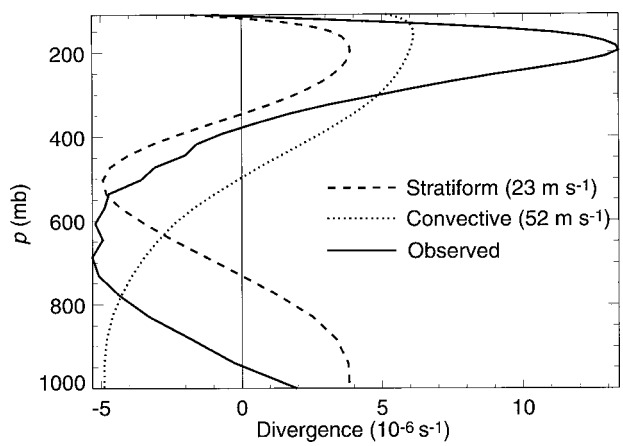

FIG. 8. Divergence measured by rawinsondes when extensive, deep convection-generated cloud systems affected the intensive flux array (centered near 2°S, 156°E) over the western tropical Pacific during TOGA COARE. Sixteen cases were used to compute the net divergence (solid curve). The components of the net divergence constituted by the 52 and 23 m s^{-1} gravity wave responses to the mass disturbance are shown by the dashed and dashed–dotted curves, respectively. [Derived from calculations of Mapes and Houze (1995) and provided by B. Mapes.]

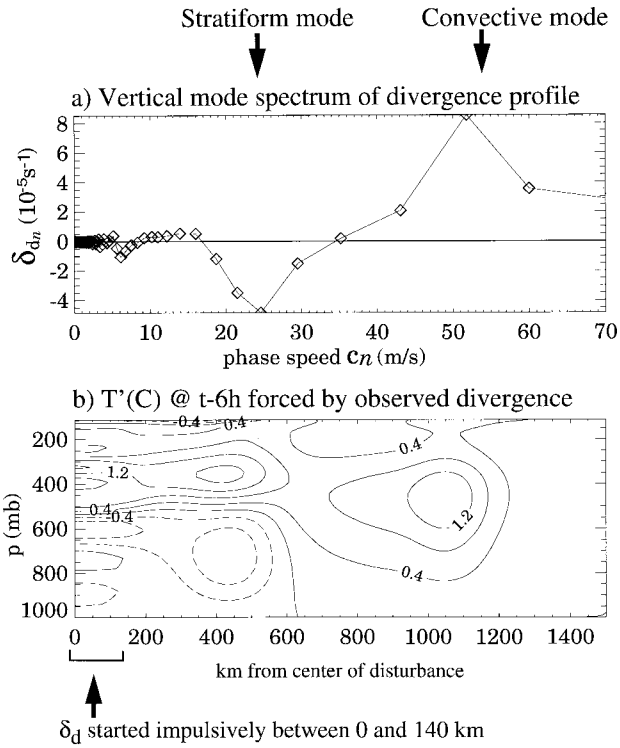

FIG. 9. Results of a linear spectral model of a large-scale tropical atmosphere perturbed by a mass divergence profile. The symbol δ_d stands for the "diabatic divergence," which is the mass disturbance produced by the net heating of a mesoscale precipitating cloud system embedded in the large-scale flow. The observed divergence profile used for δ_d is based on airborne Doppler radar and sounding observations obtained over the western tropical Pacific in TOGA COARE in regions containing large cumulonimbus cloud systems. This observed divergence profile is applied impulsively at the initial time t over a region 140 km in horizontal dimension with a horizontal $\cos^2$ profile. The model computes the response of the large-scale environment to the cloud disturbance at all times after the impulsive mass disturbance. The response is a spectrum of gravity waves with varying vertical wavelengths. Each wavelength corresponds to a wave speed c_n. The symbol δ_{dn} in (a) represents the spectral coefficient (magnitude) of the response at each wave speed. Temperature perturbation T shown by the contours in (b) is produced by the fast (convective) and slow (stratiform) gravity-wave bores 6 h after the impulsive start (time t) of the heating. [Adapted from Mapes and Houze (1995).]

Figure 8 shows the computed 52 and 23 m s^{-1} components of the divergence profile in comparison to the total observed profile of divergence. The 52 m s^{-1} component has a two-layer structure, consisting of convergence at low levels and divergence at upper levels, while the 23 m s^{-1} component has a three-layer structure, consisting of convergence at midlevels and divergence at upper and lower levels. Evidently, these two dominant modes of the observed divergence profile correspond respectively to the convective and stratiform portions of the precipitation pattern. Added together, the convective (52 m s^{-1}) and stratiform (23 m s^{-1}) curves in Fig. 8 account for nearly the entire observed divergence (solid curve).

The atmospheric adjustment to the active convective region is a fast-moving gravity wave "bore" that displaces environmental mass downward, to mass-balance the convergent inflow to the convective region at low levels and the divergent outflow aloft. Since this bore moves away at 52 m s^{-1} (over 100 mph), the adjustment is very quick. The adjustment to the stratiform region's older convection is less than half as fast, and this bore displaces mass upward in the lower troposphere and downward in the upward troposphere to adjust for the stratiform region's convergence at midlevels and divergence at upper and lower levels.

Figure 9b shows the effect of the fast (convective) and slow (stratiform) bores 6 h after the impulsive start of the heating. The convective bore has produced a mass-compensating downward displacement through the depth of the troposphere at 600–1300 km from the center of the disturbance. This compensating downward motion suppresses convection at these distances. At 150–600 km from the source, the stratiform bore, which has moved out only about half as far as the convective bore, has produced a net *upward* displacement of mass in the lower troposphere and a net downward displacement aloft. An important implication is that a deep convective tropical disturbance may actually encourage new convection in its immediate vicinity via the compensating upward motion in the lower troposphere. This result led Mapes (1993) to dub tropical convection "gregarious."

8. Convective and stratiform precipitation: A dichotomy or the ends of a spectrum?

The results of Mapes and Houze (1995) in Figs. 8 and 9 suggest that there is no reason, from the viewpoint of large-scale dynamics, to distinguish categories of air motion in a tropical precipitation region other than the categories convective and stratiform—that is, a dichotomous structure of convection. The impression formed from looking at radar-echo maps of tropical precipitation, however, is that a significant portion of the precipitation field is difficult to characterize as convective or stratiform. In an earlier paper, Mapes and Houze (1993) classified one-third of the

radar echoes observed with the WP-3D radars over the tropical ocean north of Australia as "intermediary," because the echo structure appeared to be neither obviously convective nor obviously stratiform, and because these echoes appeared to be in the process of converting from convective to stratiform structure. Mapes and Houze's (1993) findings thus suggest that a spectrum of structures exists between the convective and stratiform extremes, an apparent contradiction to the 1995 results.

The key to resolving this apparent contradiction is to keep in mind that radar-echo structure is not a single-valued function of the vertical air motions. If the intermediary radar-echo structures represented a significantly different kinematic category, the mass-divergence spectrum (Fig. 9a) would not be so decidedly bimodal. Each instantaneous two-dimensional cross section of radar data (horizontal or vertical) contains only a selected subset of the data in a three-dimensional volume. A natural tendency is to draw cross sections through extrema, which give the cross sections a rougher (more "convective") appearance. A more representative and complete way of viewing the echoes is to *combine all the data in the three-dimensional volume of space scanned by a radar in a single plot and inquire about the statistics of the radar echoes in that volume.* Yuter and Houze (1995a–c) present the radar data from a three-dimensional volume of space as a joint probability distribution, which they refer to as a "contoured frequency by altitude diagram," or CFAD. The CFAD of radar reflectivity consists of contours showing the range and relative normalized frequency of occurrence of radar reflectivity values as a function of reflectivity and height above ground.

Figure 10a shows a CFAD of the radar reflectivity values observed in a convective precipitation region of a Florida cumulonimbus. The distribution of reflectivities at all altitudes is broad, and even at high altitudes a few rather high reflectivities occur, indicating the presence of graupel or small hail, which is consistent with growth by riming in strong updrafts. In contrast, the stratiform region CFAD of a squall line in Kansas (Fig. 10c)[3] shows a narrower distribution of relatively uniform values of reflectivity at all altitudes, and at upper levels, the mode is a much lower reflectivity, consistent with a dominance of vapor deposition as the primary microphysical growth mode of the particles. The mode of the distribution increases as the altitude decreases, indicating the microphysical growth and aggregation of the falling precipitation particles as they approach the melting level. Just below the 0°C level (~4 km), the mode jumps to a high value, corresponding to the typical reflectivity of the melting aggregates falling through the layer.

As the storm within the three-dimensional volume scanned by a radar ages, the CFAD of reflectivity changes from a more convective to a more stratiform structure. Yuter and Houze (1995b) found that changeover occurred quickly, even while the storm still contained a few intense up- and downdrafts and before the storm appeared obviously stratiform in individual vertical cross sections of reflectivity. The CFAD in Fig. 10b is for a time in the mid- to late stages of the same storm whose early convective stage is represented in Fig. 10a. Although the storm still contained a wide range of vertical velocities, the reflectivity field was already *statistically* more stratiform, with a narrowing of the distribution. This result of Yuter and Houze (1995b) suggests that the intermediary radar-echo structures identified by Mapes and Houze (1993) would have been categorized as stratiform had they been viewed as CFADs.

Yuter and Houze's (1995b,c) results further indicate that even while some strong up- and downdrafts were still active, and the radar echo pattern seen in horizontal and vertical cross sections was nonuniform, most of the mass flux of the storm was in updrafts insufficiently strong to prevent ice particles from falling or to produce much liquid water to be collected by the falling ice particles. In a statistical sense, then, most of the volume of the storm was occupied by ice particles growing primarily by vapor deposition and falling relative to the ground; that is, the stratiform precipitation process dominated in most of the volume of the storm even though some spots within the storm still had strong updrafts.

Mapes and Houze (1993) used a large set of airborne Doppler-radar measurements to determine the vertical profiles of divergence in the convective, intermediary, and stratiform radar echo structures they observed over the tropical ocean north of Australia

[3]Figure 10c is not from the same case as (a) and (b), because the observations in the Florida case illustrated in (a) and (b) ended before the fully developed stratiform region could be observed. The convective region of the Kansas case illustrated in (c) could not be used for (a) and (b) because the spatial resolution of the radar data in the Kansas case was too coarse to show the detailed structure of the convective region. Hence, Fig. 10 had to be pieced together from the two cases.

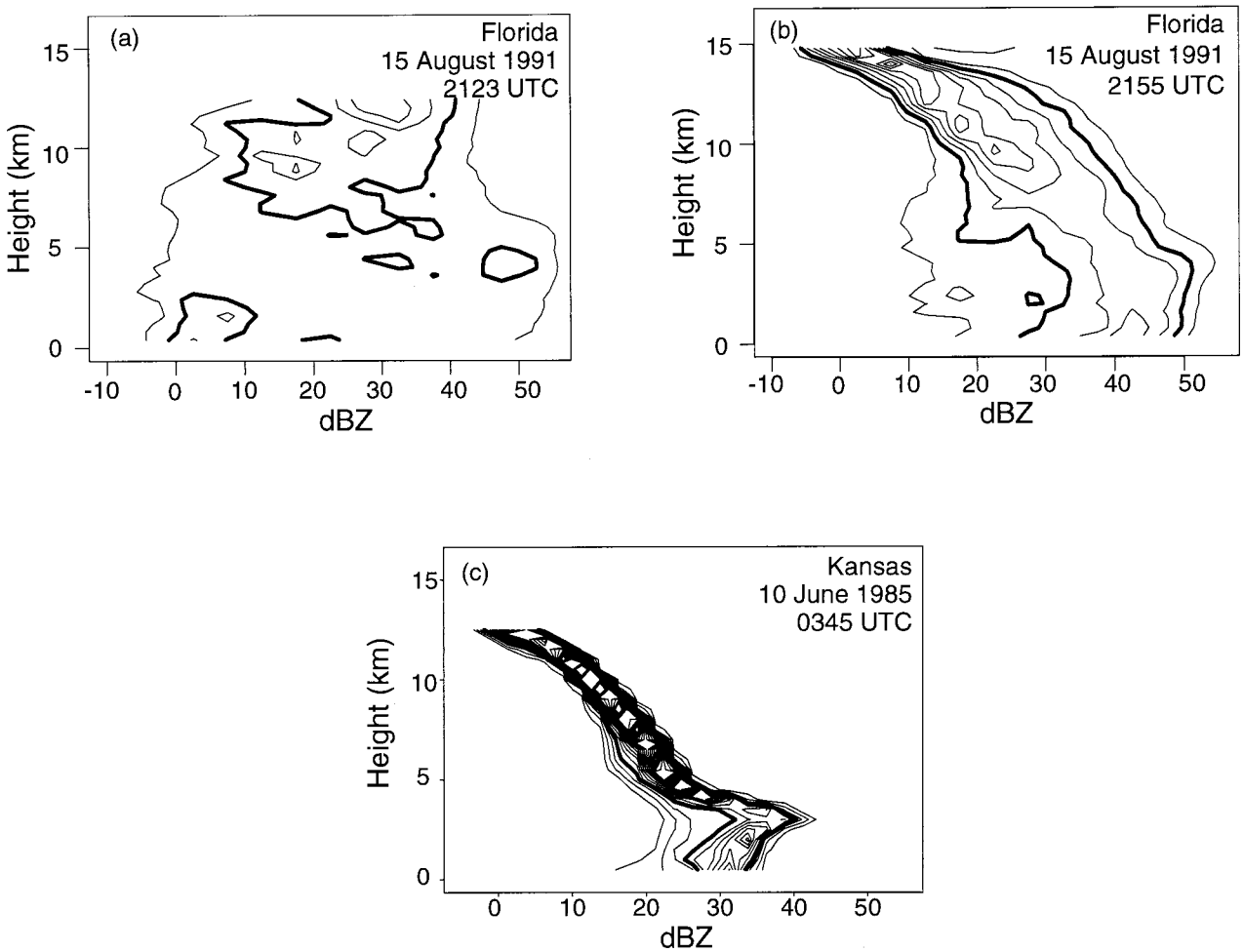

FIG. 10. Examples of CFADS of reflectivity for (a) region of young, vigorous convection; (b) a region of intermediary convection; and (c) a stratiform precipitation region. Units of contours are (frequency of occurrence, in percent of observations at a given altitude)/(*dz* *d*dBZ), where *dz* = 0.4 km and *d*dBZ = 5. Contours are drawn at intervals of 2.5% dBZ^{-1} km^{-1}. The 5% dBZ^{-1} km^{-1} contour is highlighted. [Adapted from Yuter and Houze (1995b).]

(Fig. 11). Around intermediary echo structures, they found divergence in low to midlevels overlain by a layer of convergence (Fig. 11b).[4] This behavior is further evidence that the intermediary echo regions were kinematically more like stratiform than convective precipitation regions. However, the layer of convergence was at a somewhat higher altitude than in the stratiform regions (cf. Figs. 11b,c). This difference may have been a result of sampling (the data in Fig. 11b were not necessarily obtained in the same storms as the data in Fig. 11c), or there may be a slight difference between intermediary and stratiform dynamics.

Figure 12 suggests possible relationships between the pattern of up- and downdrafts and the corresponding divergence profiles during the various stages of convection. In regions dominated by active convection (Fig. 1a), strongly buoyant, undiluted elements rise, and mass continuity requires that the buoyant elements be surrounded by a pressure-gradient force field, which pushes air out of the path of the top of the cell and in toward the base of the buoyant updraft in the lower

[4]All the profiles in Fig. 11 should have a layer of divergence at upper levels. The sensitivity of the radar used to obtain the divergence profiles in Fig. 11 was, however, not sufficient to observe the low intensity of the reflectivity at these high levels. Other data showed that the actual cloud tops were several kilometers above the 200-mb level (~12 km), which is the highest level at which the divergence could be reliably measured by the radar. All the mean profiles showed a net convergence below 12 km. On the linear pressure scale used in Fig. 11, the areas under the divergence profiles are proportional to mass divergence. Since mass convergence and divergence must balance over a full vertical column, the net convergence seen in Fig. 11 implies that the higher levels must have been characterized by net divergence in all three cases.

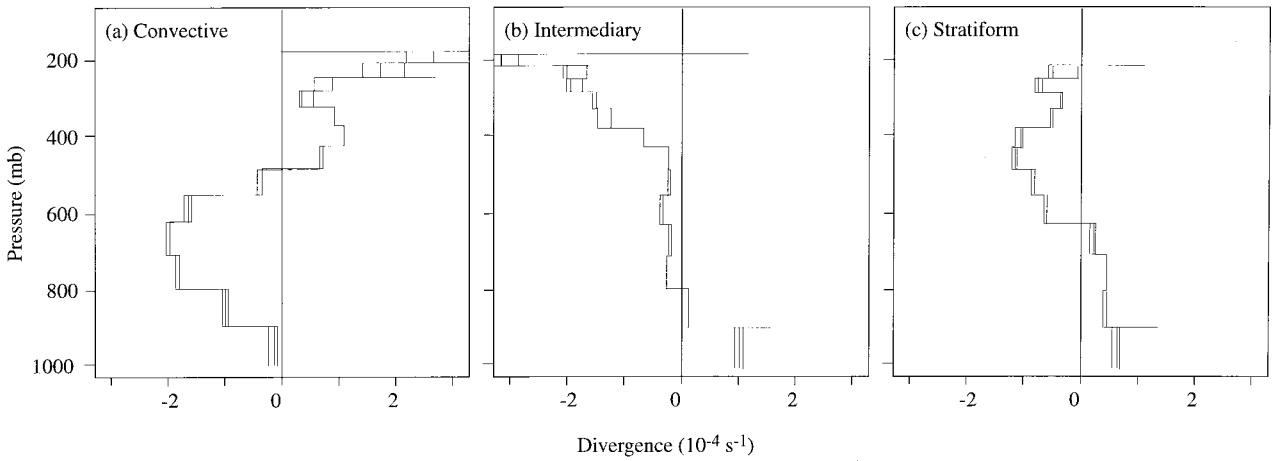

FIG. 11. Mean divergence observed by airborne Doppler radar in tropical precipitating cloud systems over the ocean north of Australia. [Adapted from Mapes and Houze (1993).]

troposphere. In a region containing one or more active, deep convective elements, both positively buoyant updrafts and negatively buoyant downdrafts are present in the lower troposphere (Fig. 12a). Over the region of convection, the upward vertical mass flux of the updrafts dominates over the downward mass flux of the downdrafts. In the boundary layer, some of the convergence into the base of the buoyant updrafts is canceled, in an area-averaged sense, by divergence associated with downdrafts. Thus, the maximum convergence into the convective region of a mesoscale convective system is usually found at some height above the boundary layer. Even so, the convective-region divergence profile is *two layered,* with the lower troposphere characterized by net convergence and the upper troposphere by net divergence.

As a strongly buoyant element rises in a cumulonimbus cloud, it typically gets cut off from its supply of high moist-static energy air from below. When it reaches the stable tropopause, it spreads out, collapsing into a flattened buoyant element (Lilly 1988). The convergence produced by the pressure-gradient force at the base of the buoyant element is then elevated into

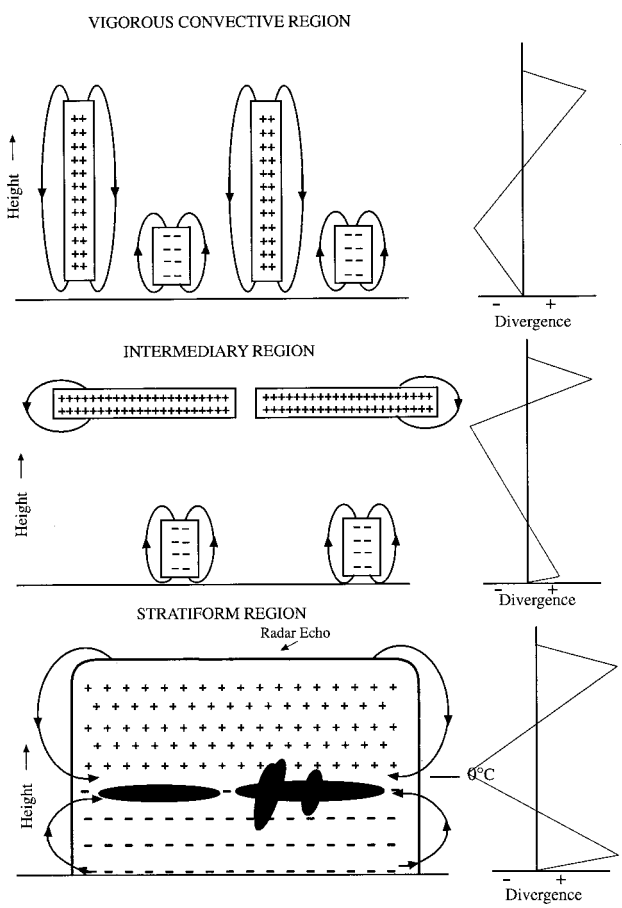

FIG. 12. Conceptual models explaining the vertical profiles of divergence in regions of precipitation dominated by (a) young, vigorous convection; (b) intermediary convection; and (c) stratiform precipitation. In (a) and (b), the rectangles enclose regions of positive (+) and negative buoyancy (–) associated with up- and downdrafts, respectively. The arrowheads indicate the direction of the pressure-gradient force field induced by the buoyancy field [see Fig. 7.1 of Houze (1993).] The divergence profiles on the right-hand sides of (a) and (b) reflect the net effect of these force fields. In (c), no attempt is made to identify individual buoyant or negatively buoyant elements, as the precipitation (outlined by the radar-echo boundary) contains the remains of previously vigorous buoyant and negatively buoyant elements, which intermingle such that the upper levels are generally positively buoyant, and the lower levels are generally negatively buoyant. The heavy shading in (c) indicates the bright band just below the 0°C level and the remnants of old cells distorted into fall streaks by the wind shear.

the upper troposphere. Figure 12b suggests that an intermediary echo region, of the type analyzed by Mapes and Houze (1993), is dominated at upper levels by buoyant elements at this stage of development and at lower levels by negatively buoyant downdrafts. The net profile of divergence in a region of intermediary echo structure would then look like that on the right-hand side of Fig. 12b, with a layer of maximum convergence in the upper troposphere corresponding to the convergence at the base of the elevated, horizontally spreading buoyant elements. This hypothetical profile of divergence is consistent with the observed divergence profile in intermediary regions (Fig. 11b).

In the stratiform region, negatively buoyant downdrafts dominate the lower troposphere, while weakened, but still positively buoyant updrafts, dominate the upper troposphere, and a strong melting layer produces a radar bright band in the middle troposphere (Fig. 1b). By this time, a lot of individual buoyant elements have risen into the upper troposphere, reached their level of zero buoyancy, and spread laterally. Some reach the tropopause, but others entrain and come to rest at lower levels. The net result is that the whole mid- to upper troposphere above the melting layer is filled with intermingled old buoyant elements (Fig. 12c). At this stage, no strongly buoyant elements dominate the mean buoyancy; rather, the conglomeration of old elements dominates the picture. So Fig. 12c shows the mid- to upper levels as generally positively buoyant but does not attempt to identify individual elements.

A general region of negative buoyancy dominates the stratiform region from the 0°C level down to the earth's surface (Fig. 12c). This region of negative buoyancy, in a mature stratiform region, is a combination of old negatively buoyant convective elements, cooling of the air in the melting layer, and entrainment of low moist-static-energy air from midlevels of the environment. The pressure force field required by the residual positive buoyancy aloft and the negative buoyancy of both the downdrafts and the melting layer lead to a maximum of convergence just above the 0°C level.

By comparing the divergence profiles in Figs. 12b and 12c, we infer that they differ only in the altitude of the maximum convergence into the region, which is slightly higher in the intermediary case. Thus, while on the order of one-third of the reflectivity patterns have an intermediary appearance in two-dimensional cross sections of reflectivity fields (Mapes and Houze 1993), the air motions in the intermediary and stratiform stages have qualitatively similar divergence profiles, characterized by a mid- to upper-level layer of convergence sandwiched between upper and lower divergence layers. This *three-layered* structure differs fundamentally from the two-layered structure seen in the convective region (Fig. 12a). The three divergence profiles sketched in Figs. 12a–c are entirely consistent with the three observed profiles in Figs. 11a–c. From this we infer that the intermediary and stratiform profiles both contribute to the slow mode of atmospheric response identified by Mapes and Houze (1995, Fig. 9), while the convective region profiles (Fig. 11a) contribute to the fast mode. To put it another way, the first-order dynamical distinction to be made in evaluating a tropical convective precipitation system is between actively convective portions (like Fig. 11a) and all other intermediary and stratiform portions, which contain old convective elements and well-developed stratiform rain.

9. Implications for identifying convective and stratiform precipitation

Because precipitation is a measure of the latent heat of condensation released into the air, and since heat is the result of upward air motion, the precipitation field is diagnostic of the rearrangement of the mass field by tropical convection. This relationship of the heating and mass fields to the precipitation field is a primary motivation of the Tropical Rainfall Measuring Mission (TRMM; Simpson 1988). It is now evident that the large-scale mass field responds primarily to the two-layered mass divergence profile in convective precipitation regions and the three-layered profile in stratiform and intermediary precipitation regions. To use the precipitation field diagnostically, it is necessary to separate the convective component of the precipitation from the remainder. This exercise, while often referred to as "convective/stratiform separation," is simply to separate the convection portion of the precipitation from the remainder of the precipitation. For this reason, convective/stratiform separation methods that seek the stratiform component first and assign the remainder of the precipitation to the convective category are risky since they are likely to combine the intermediary precipitation (with its three-layered mass divergence profile) with the convective (two-layered mass divergence profile) to produce a kinematically nonuniform category of rainfall.

Figure 13 illustrates a method (Churchill and Houze 1984; Steiner et al. 1995; Yuter and Houze 1997a,b)

that seeks the convective precipitation first and assigns the remainder to the "stratiform" category (which should really be called stratiform *plus* intermediary). Each pixel of a Cartesian reflectivity field is examined and declared a convective center if it exceeds a prescribed threshold of reflectivity or if it exceeds the reflectivity in a region surrounding the pixel (~ 10 km in diameter) by a specified factor, which increases as the reflectivity at the convective center decreases. If a pixel is declared a convective center, then a 4–5-km diameter region surrounding the convective center is defined as convective precipitation. There is no attempt to define a convective region smaller than 4–5 km in diameter. Often several convective centers are close together and the convective regions overlap, and the union of these convective areas may define a contiguous region of convective precipitation tens to even hundreds of kilometers across. Thus, the separation method does not attempt to identify individual up- and downdraft regions, which may be smaller in scale than 4–5 km, but rather attempts to delineate general regions in which active convection, like that idealized in Fig. 1a, predominates and hence has a mass divergence profile like that in Fig. 12a.

The method illustrated by Fig. 13 is very practical because it is applied to the reflectivity field alone. It does not assume any direct knowledge of the in-cloud air motions. The basic premise of the method is that if the reflectivity field is either very intense or pockmarked with cores of intense reflectivity, then the air motions must be more like those in Fig. 1a than those in Fig. 1d. Steiner et al. (1995) and T.-C. Chen (1996, personal communication) have tested this convective/stratiform separation method on datasets for which high-resolution dual-Doppler radar measurements provided simultaneous measurements of the vertical velocity and radar reflectivity so that the vertical velocity data could be used as an independent test of the convective/stratiform separation. They first determined the convective and stratiform regions by applying the method to the reflectivity field. Then they examined CFADs of the vertical velocity in these regions. The statistics of the vertical velocity showed that the air motions in the regions designated convective had a wide distribution of vertical velocities, with peaks > ~ 10 m s^{-1}. In the regions that the algorithm designated stratiform, the distribution was narrow, with practically no vertical velocities exceeding 2 m s^{-1} in absolute value, with most of the values < 1 m s^{-1}. These statistics confirm that the air motions in the regions identified as convective by the reflectivity algorithm were like those of Fig. 1a, while the air motions in the stratiform regions were like those of Fig. 1d. More tests of this type are needed.

10. Conclusions

In extratropical cyclones, lifting of air is generally widespread and weak, the precipitation produces layered radar echoes, and the precipitation is traditionally called "stratiform."[5] This conceptual model contrasts with that of convective "cells," which are vertically oriented cores of high reflectivity, embedded in cumulonimbus, which form as a product of free convection driven by buoyancy. When radar observations in the Tropics in the early 1970s showed stratiform radar echoes alongside convective cells, a paradox arose: stratiform precipitation, thought previously to be a product of widespread stable lifting, was falling from tropical cumulonimbus clouds as a product of buoyant convection. Stratiform precipitation and convection could no longer be viewed as mutually exclusive.

This paper suggests resolving this paradox by using the noun *convection* to describe the overturning of the atmosphere that is required to neutralize the vertical distribution of moist static energy—just as convection in an incompressible fluid neutralizes an unstable vertical distribution of density—and by using the adjectives *convective and stratiform* to describe the different types of precipitation seen within a given region of convection-generated cumulonimbus.

Within a region of precipitation where the convection is young and vigorous, strong updrafts produce cells of heavy rain, seen on radar as locally vertically

[5]There are several exceptions to the generally stratiform nature of frontal precipitation. The stratiform precipitation often contains weak embedded convective cells, often confined to a potentially unstable layer aloft. Release of conditional symmetric instability within the stratiform cloud mass may lead to embedded lines of somewhat heavier precipitation. Embedded cells aloft and lines of release of conditional symmetric instability do not change the fundamentally stratiform nature of the precipitation but, rather, give it a texture. Sometimes, however, the frontal cloud system contains a "narrow cold frontal rainband," in which strong, convective-like air motions are forced by the convergence along the surface wind-shift line. The narrow cold-frontal band is usually embedded in a much broader region of predominantly stratiform clouds and precipitation. Sometimes the frontal convergence triggers a squall line, in which a deep layer of instability in the warm air is released by the frontal lifting and leads to convective air motions that dominate over and replace the frontal air motions. For further details, see chapter 11 of Houze (1993).

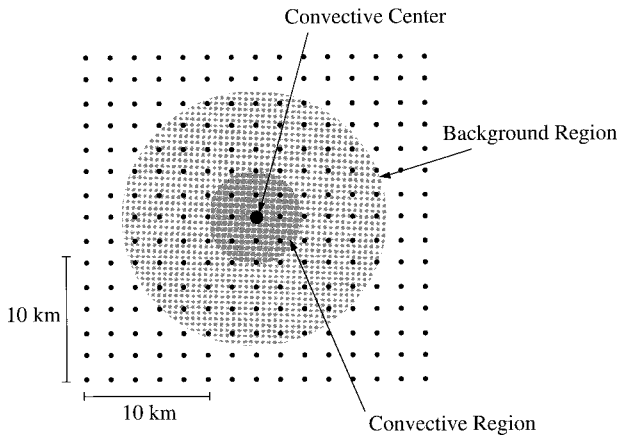

FIG. 13. Schematic illustrating a method for separating the convective component of precipitation from the rest of the precipitation. The illustration assumes a 2-km Cartesian grid spacing for the data points; however, the method may be applied at different resolutions and could be adapted to polar coordinates. The algorithm examines the reflectivity at each grid point. If that reflectivity exceeds some prescribed high value, or if it exceeds the mean reflectivity in a "background region" (lightly shaded region, ~ 10 km in diameter) surrounding the point by some specified amount, the point is declared a convective center. If the point is declared a convective center, then that point and all the points in a small region (~ 4–5 km in diameter) surrounding the convective center constitute a "convective region" centered on the point. This exercise is repeated for each data point in the grid and the union of all the convection regions makes up the total convective precipitation region. [Adapted from Steiner et al. (1995).]

oriented cells of high reflectivity (Figs. 1a–c). Within a region of precipitation where the convection is older and much less vigorous, a residual population of weakened updrafts and downdrafts produces precipitation that appears stratiform on radar (Figs. 1d–f). As vigorous cells weaken, they pass through an intermediary stage of development, when two-dimensional cross sections of radar data are ambiguous but statistics of the reflectivity and vertical air velocity in a three-dimensional volume of space indicate that the radar echoes are basically stratiform; that is, they have a narrow distribution of reflectivity with a vertical distribution suggestive of precipitation particles growing mainly by vapor deposition and vertical velocities $< \sim 1$ m s^{-1}. In contrast, the statistics of the echoes in a three-dimensional volume containing young, vigorous convection show a broad distribution of reflectivity. Particles there appear to be able to grow by collection (coalescence and riming), which accounts for the existence of high reflectivities in the outliers of the reflectivity distribution. Statistics of the air motions confirm that while most of the vertical velocities in the convective regions are relatively small, there are a few large vertical velocities ($> \sim 2$ m s^{-1}) capable of carrying particles upward and generating high cloud liquid water contents for the growing particles to collect.

Large-scale dynamics of the tropical atmosphere are profoundly affected by cumulonimbus clouds. However, the effects of the clouds upon the atmosphere are distinctly subdivided such that part of the atmospheric response derives from the young vigorous convective precipitation areas, characterized by radar echoes in the form of cells, while another part derives from the older weaker part of the convection, where the precipitation echoes are intermediary and stratiform. The young, vigorous cells induce an atmospheric response that is two layered, with air converging into the active convection at low levels and diverging aloft. The older, weaker intermediary and stratiform precipitation areas induce a three-layered response, in which the environment converges into the weak precipitation area at midlevels and diverges out from it at lower and upper levels.

These results suggest that it is important to separate the convective precipitation from all the rest for two reasons:

1) The microphysical growth processes at work in the convective precipitation areas are profoundly different from those in the intermediary and stratiform precipitation areas. In convective precipitation areas, precipitation particles increase their mass primarily by collection of cloud water (coalescence and/or riming). In intermediary and stratiform precipitation areas, the precipitation particles increase their mass by vapor diffusion. If high-resolution numerical prediction models are to forecast accurately the location, amount, and type of precipitation, they must represent (either parametrically or explicitly) the microphysical growth processes accurately. Radar data can validate these models only if the echoes are accurately subdivided to separate the active vigorous convective echoes from the remainder of the precipitation.
2) Global climate and circulation models must simulate the role of convection accurately. To validate such models, satellite observational programs such as TRMM (Simpson 1988) are attempting to map the precipitation over the globe three dimensionally. Instrumentation in TRMM will determine the vertical as well as the horizontal structure of pre-

cipitation throughout the Tropics. The primary goal is to use this information to determine the four-dimensional (i.e., temporal and spatial) patterns of latent heating over the whole Tropics. Algorithms applied to the TRMM data will attempt to identify the two principal modes of heating, by separating the convective component of the precipitation, and hence the associated heating, from the remainder. The success of TRMM will hinge on the accuracy of this separation.

From 1) and 2) above, it is clear that the distinction between young convective precipitation and older stratiform precipitation in convection-generated clouds is important in order to forecast precipitation accurately and to evaluate the effects of tropical convection on the global circulation. These applications are of great practical significance. The processes represented in Fig. 1 remain, however, without much quantitative documentation. If models for numerical prediction and climate simulation are going to improve, these processes must be measured and quantified. The only viable way to do this is to mount field projects that can determine the dynamical and microphysical processes on space and time resolutions adequate to resolve individual convective cells and distinguish unambiguously the major cloud microphysical mechanisms, especially at all altitudes above the 0°C level. For these projects, instrumentation and observational platforms must be developed to improve on our current capabilities to measure vertical air motion, water vapor, temperature, pressure, and ice and liquid particle mass, shapes, and concentrations. Without such empirical improvements in our knowledge base, it is hard to foresee real progress in the ability to model processes in the atmosphere that are sensitive to convective and stratiform precipitation processes in cumulonimbus clouds.

Acknowledgments. This paper is based on the author's presentation to the Tropical Rainfall Measuring Mission U.S. Science Team Meeting, Greenbelt, Maryland, July 1996. The author benefited greatly from the comments of Dr. Pauline Austin, Professor Colleen Leary, Dr. Brian Mapes, Professor Bradley Smull, and Dr. Sandra Yuter. Candace Gudmundson edited the manuscript and Kay Dewar drafted some of the figures. This research has been supported by NOAA Cooperative Agreement NA67RJ0155 (JISAO Contribution 351), National Science Foundation Grant ATM-9409988, and NASA Award NAGS-1599.

References

Battan, L. J., 1973: *Radar Observations of the Atmosphere.* University of Chicago Press, 324 pp.

Braun, S. A., and R. A. Houze Jr., 1995: Melting and freezing in a mesoscale convective system. *Quart. J. Roy. Meteor. Soc.*, **121A,** 55–77.

Bretherton, C. S., and P. K. Smolarkiewicz, 1989: Gravity waves, compensating subsidence, and detrainment around cumulus clouds. *J. Atmos. Sci.,* **46,** 740–759.

Byers, H. R., and R. R. Braham Jr., 1949: *The Thunderstorm*. U.S. Government Printing Office, 287 pp.

Cheng, C.-P., and R. A. Houze Jr., 1979: The distribution of convective and mesoscale precipitation in GATE radar echo patterns. *Mon. Wea. Rev.*, **107,** 1370–1381.

Churchill, D. D., and R. A. Houze Jr., 1984: Development and structure of winter monsoon cloud clusters on 10 December 1978. *J. Atmos. Sci.,* **41,** 553–574.

Hobbs, P. V., 1974: *Ice Physics.* Oxford Press, 837 pp.

Houghton, J. G., 1968: On precipitation mechanisms and their artificial modification. *J. Appl. Meteor.*, **7,** 851–859.

Houze, R. A., Jr., 1975: Squall lines observed in the vicinity of the researcher during phase III of GATE. Preprints, *16th Radar Meteorology Conf.*, Houston, TX, American Meteorological Society, 206–209.

——, 1977: Structure and dynamics of a tropical squall-line system. *Mon. Wea. Rev.*, **105,** 1540–1567.

——, 1989: Observed structure of mesoscale convective systems and implications for large-scale heating. *Quart. J. Roy. Meteor. Soc.*, **115,** 425–461.

——, 1993: *Cloud Dynamics.* Academic Press, 573 pp.

——, and D. D. Churchill, 1987: Mesoscale organization and cloud microphysics in a Bay of Bengal depression. *J. Atmos. Sci.,* **44,** 1845–1867.

——, B. F. Smull, and P. Dodge, 1990: Mesoscale organization of springtime rainstorms in Oklahoma. *Mon. Wea. Rev.*, **118,** 613–654.

Huschke, R. E., 1959: *Glossary of Meteorology.* Amer. Meteor. Soc., 638 pp.

Leary, C. A., 1984: Precipitation structure of the cloud clusters in a tropical easterly wave. *Mon. Wea. Rev.*, **112,** 313–325.

——, and R. A. Houze Jr., 1979a: The structure and evolution of convection in a tropical cloud cluster. *J. Atmos. Sci.*, **36,** 437–457.

——, and ——, 1979b: Melting and evaporation of hydrometeors in precipitation from anvil clouds of deep tropical convection. *J. Atmos. Sci.,* **36,** 669–679.

LeMone, M. A., and E. J. Zipser, 1980: Cumulonimbus vertical velocity events in GATE. Part I: Diameter, intensity, and mass flux. *J. Atmos. Sci.,* **37,** 2444–2457.

Lilly, D. K., 1988: Cirrus outflow dynamics. *J. Atmos. Sci.,* **45,** 1594–1605.

Mapes, B. E., 1993: Gregarious tropical convection. *J. Atmos. Sci.,* **50,** 2026–2037.

——, and R. A. Houze Jr., 1993: Cloud clusters and superclusters over the oceanic warm pool. *Mon. Wea. Rev.,* **121,** 1398–1415.

——, and ——, 1995: Diabatic divergence profiles in western Pacific mesoscale convective systems. *J. Atmos. Sci.,* **52,** 1807–1828.

Marshall, J. S., 1953: Frontal precipitation and lightning observed by radar. *Can. J. Phys.*, **31,** 194–203.

Riehl, H., 1979: *Climate and Weather in the Tropics.* Academic Press, 611 pp.

Rutledge, S. A., and R. A. Houze Jr., 1987: A diagnostic modeling study of the trailing stratiform region of a midlatitude squall line. *J. Atmos. Sci.*, **44,** 2640–2656.

——, and D. R. MacGorman, 1988: Cloud-to-ground lightning in the 10–11 June 1985 mesoscale convective system observed during Oklahoma–Kansas PRE-STORM. *Mon. Wea. Rev.*, **116,** 1393–1408.

Shupiatsky, A. B., A. I. Korotov, V. D. Menshenin, R. S. Pastushkov, and M. Jovasevic, 1975: Radar investigations of evolution of clouds in the eastern Atlantic. GATE Rep. 14, Vol. II, International Council of Scientific Unions/World Meteorological Organization, 177–187. [Available from WMO, Case Postale 2300, CH-1211, Geneva 2, Switzerland.]

——, ——, and R. S. Pastushkov, 1976a: Radar investigations of the evolution of clouds in the East Atlantic, in *TROPEX-74. Atmosphere* (in Russian), Vol. 1, Gidrometeoizdat, 508–514.

——, G. N. Evseonok, and A. I. Korotov, 1976b: Complex investigations of clouds in the ITCZ with the help of satellite and ship radar equipment, in *TROPEX-74. Atmosphere* (in Russian), Vol. 1, Gidrometeoizdat, 508–514.

Simpson, J., 1988: TRMM: A satellite mission to measure tropical rainfall. NASA, 94 pp. [Available from Goddard Space Flight Center, Code 912, Greenbelt, MD 20771.]

Steiner, M., R. A. Houze Jr., and S. E. Yuter, 1995: Climatological characterization of three-dimensional storm structure from operational radar and rain gauge data. *J. Appl. Meteor.*, **34,** 1978–2007.

Yuter, S. E., and R. A. Houze Jr., 1995a: Three-dimensional kinematic and microphysical evolution of Florida cumulonimbus. Part I: Spatial distribution of updrafts, downdrafts, and precipitation. *Mon. Wea. Rev.*, **123,** 1921–1940.

——, and ——, 1995b: Three-dimensional kinematic and microphysical evolution of Florida cumulonimbus. Part II: Frequency distributions of vertical velocity, reflectivity, and differential reflectivity. *Mon. Wea. Rev.*, **123,** 1941–1963.

——, and ——, 1995c: Three-dimensional kinematic and microphysical evolution of Florida cumulonimbus. Part III: Vertical mass transport, mass divergence, and synthesis. *Mon. Wea. Rev.*, **123,** 1964–1983.

——, and ——, 1997a: Measurements of raindrop size distribution over the Pacific warm pool and implications for *Z–R* relations. *J. Appl. Meteor.*, **36,** 847–867.

——, and ——, 1997b: Natural variability of precipitating clouds over the western Pacific warm pool. *Quart. J. Roy. Meteor. Soc.*, in press.

Zipser, E. J., and M. A. LeMone, 1980: Cumulonimbus vertical velocity events in GATE. Part II: Synthesis and model core structure. *J. Atmos. Sci.*, **37,** 2458–2469.